

Supporting information

Modular photoorigami-based 4D manufacturing of vascular junction elements

Arpan Biswas¹, Indra Aspite¹, Sabine Rosenfeldt², Ivita Bite³, Virginija Vitola³ and Leonid Ionov^{1,*}

¹Faculty of Engineering Sciences and Bavarian Polymer Institute, University of Bayreuth, Bayreuth 95447, Germany

²Faculty of Biology, Chemistry and Earth Sciences, University of Bayreuth, Bayreuth 95447, Germany

³Institute of Solid State Physics, University of Latvia, Kengaraga St. 8, Riga, LV-1063, Latvia.

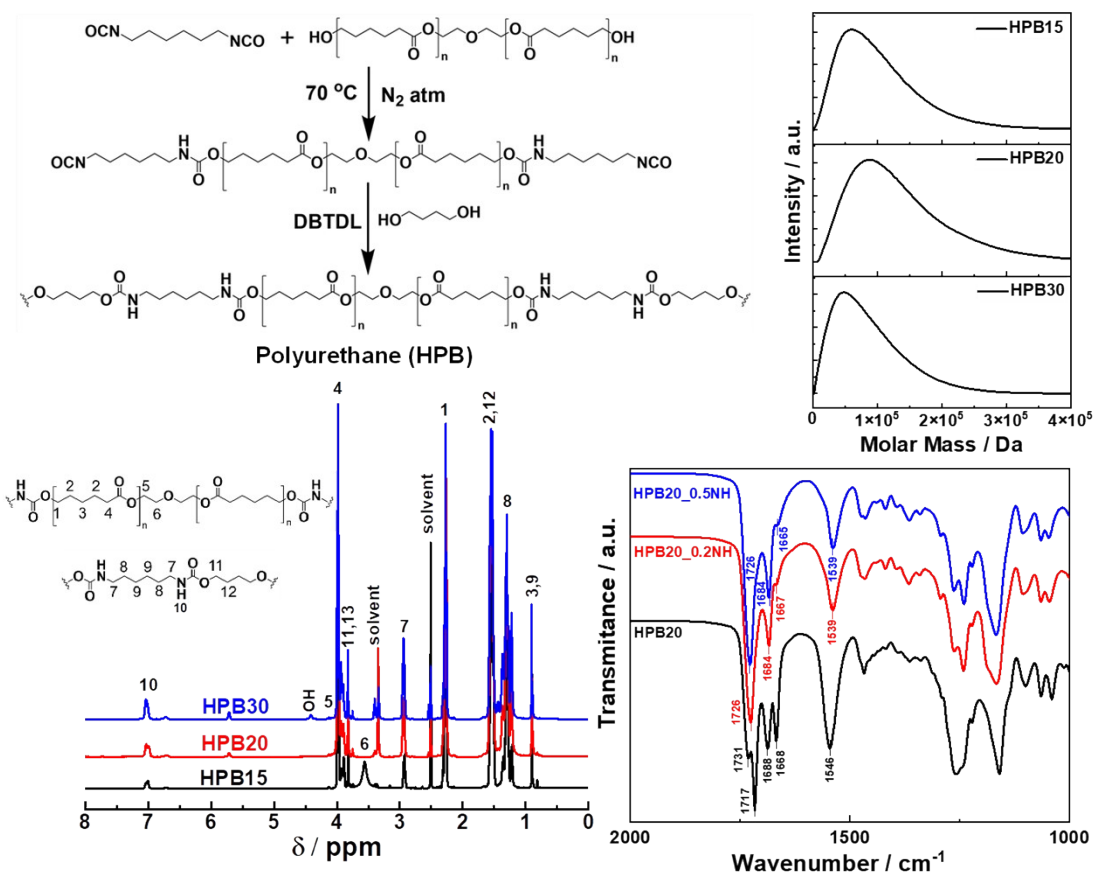


Figure S1: Synthesis and characterization of different SMPUs and nanohybrids: **a)** Schematic representation of the synthesis of SMPUs with different hard segment contents (HSC); **b)** Molar mass distribution of different synthesized PCL-PU copolymers measured using gel permeable chromatography (GPC), showing unimodal distribution; **c)** $^1\text{H-NMR}$ spectra of different synthesized PCL-PU copolymers; **d)** FT-IR spectra of different nanohybrids. The shifting of the peaks in the nanohybrids towards lower wavenumbers indicates the interaction between NPs and polymer chains.

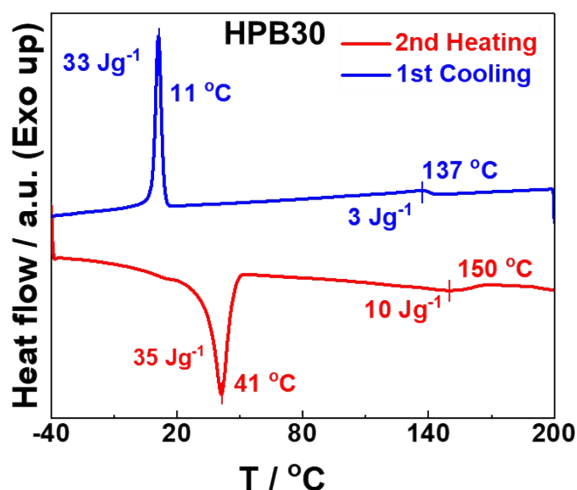


Figure S2: DSC thermogram of SMPU of 30% HSC (HPB30) showing melting and crystallization of soft segment (lower temperature) and hard segment (higher temperature) with heating-cooling cycle.

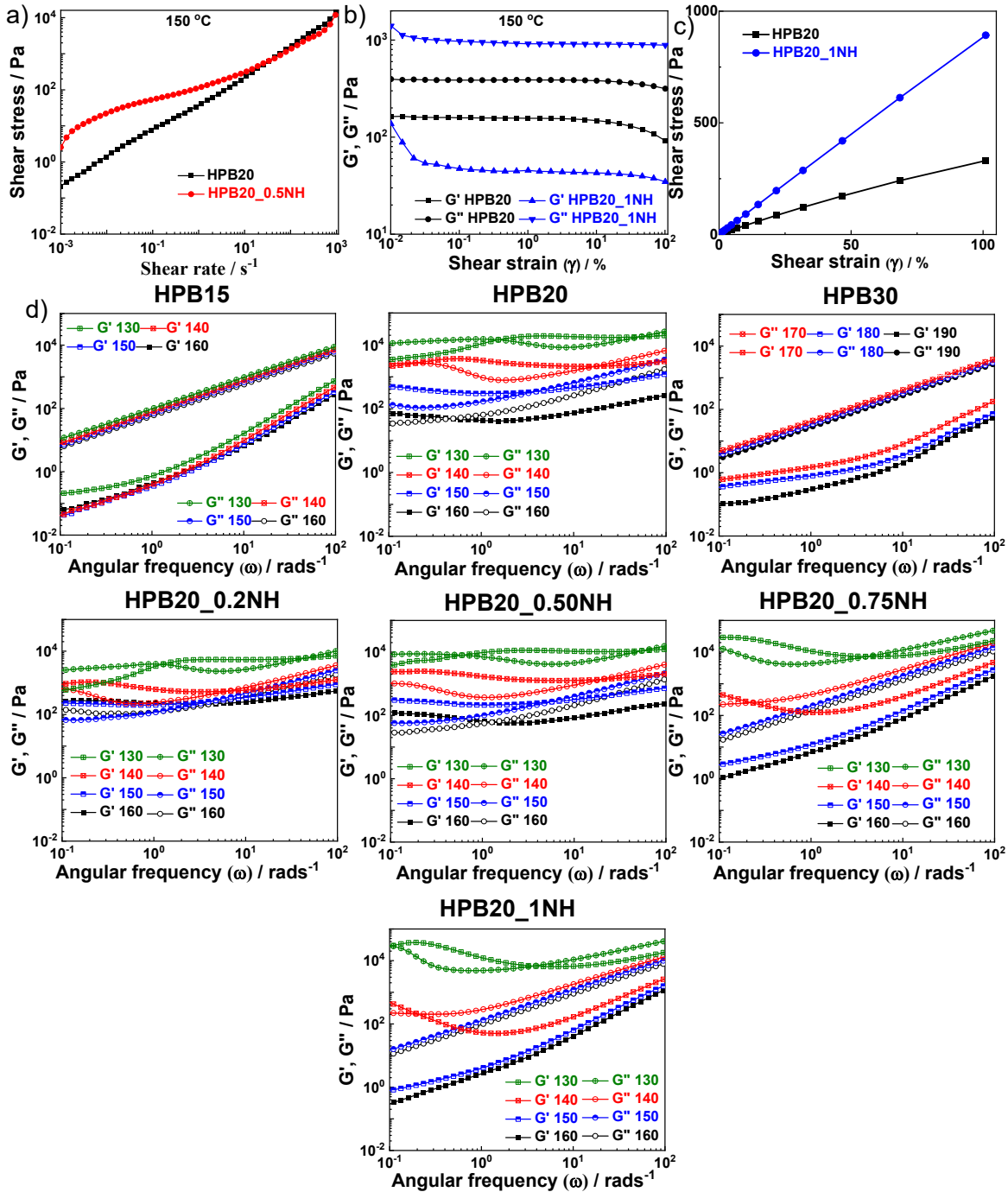


Figure S3: Rheological properties: a) Shear stress is increasing with increasing the shear rate for both pure HPB20 and its nanohybrid at 150 °C; b) In amplitude sweep at 150 °C, the storage and loss moduli remain linear with increasing shear strain and started to decrease after 13% of shear

stain; c) While the shear stress increases linearly with increasing the shear strain for both pure HPB20 and its nanohybrid (HPB20_0.5NH) at 150 °C; d) In frequency sweep, the change in storage and loss moduli has been investigated with increasing frequency at different temperatures above the melting temperature of the SMPUs and nanohybrids.

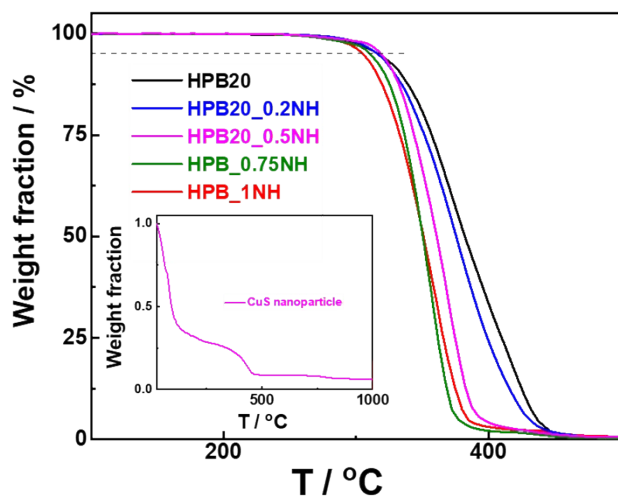


Figure S4: The thermal stability of HPB20 and nanohybrids have been investigated using thermogravimetric analysis. The temperature for 5% degradation of the polymers is considered as degradation temperature. The thermal degradation curve for CuS-PVP NPs is shown in the inset.

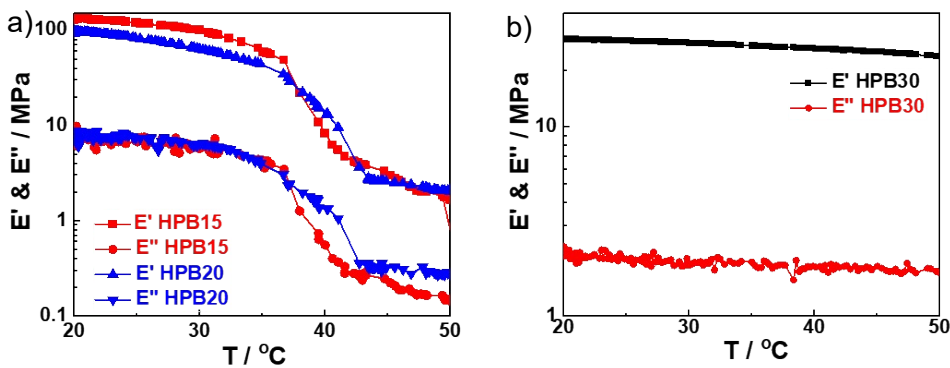


Figure S5: a) Dynamic mechanical analysis of HPB15 and HPB20 with increasing temperature and at constant frequency 1Hz reveals a sudden drop in elastic and loss moduli within the

temperature range of 30-40 °C; while no significant change in moduli is observed for b) HPB30 with that temperature range.

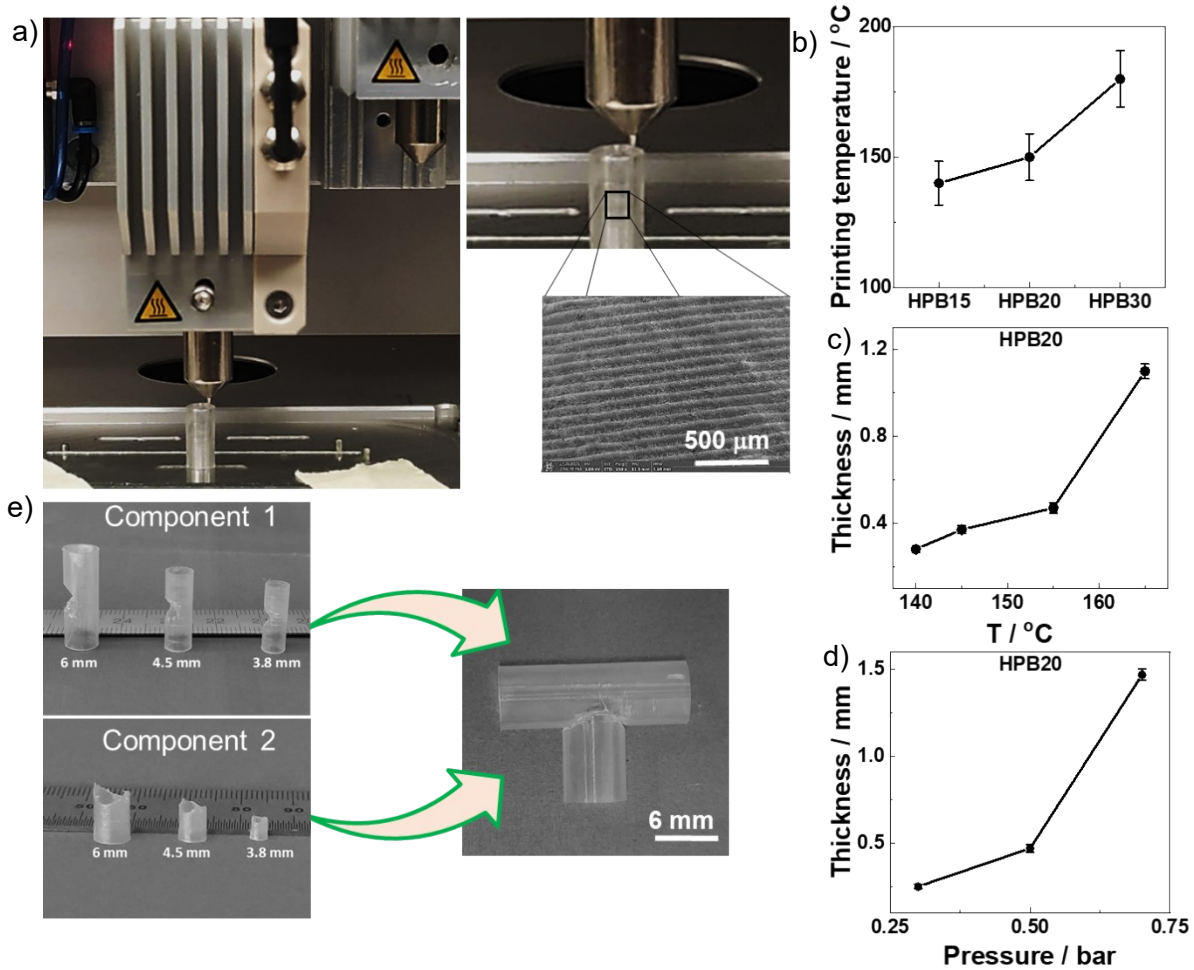


Figure 6: Fabrication of tubular components of T junction: a) 3D printing of different SMPUs and nanohybrids using a commercially available pneumatic pressure-assisted melt-extrusion-based 3D printer; b) The increase in the printing temperature of SMPUs with increasing the hard segment content (%) because of the increment in the melting temperature with higher HSC; c) and d) The thickness of the printed components increases with increasing the printing temperature and pressure for a particular SMPU because of the higher flow behavior of the polymers with increasing temperature and pressure; e) 3D printed components of the T-junction of different

diameters. It is possible to construct a T-junction with different diameters by combining component 1 and component 2 of different diameters.

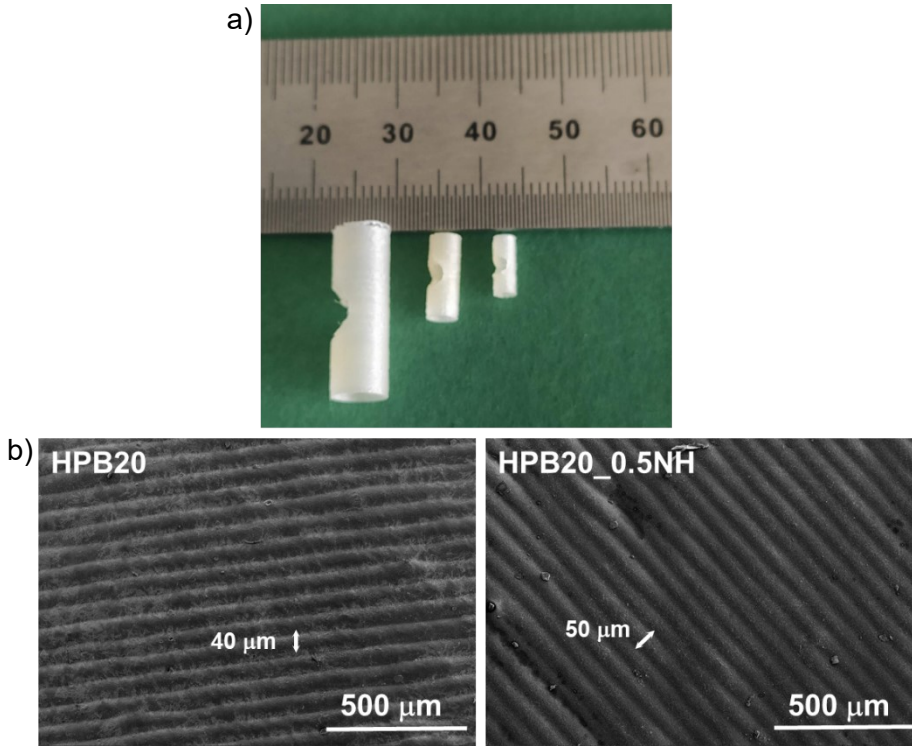


Figure S7: Characterization of 3D printed elements: a) 3D printed component 1 of the T-junction with different diameters. The smallest achievable diameter is 2 mm with a 350 μm nozzle; b) The surface morphology of the 3D printed components has been investigated with a scanning electron microscope.

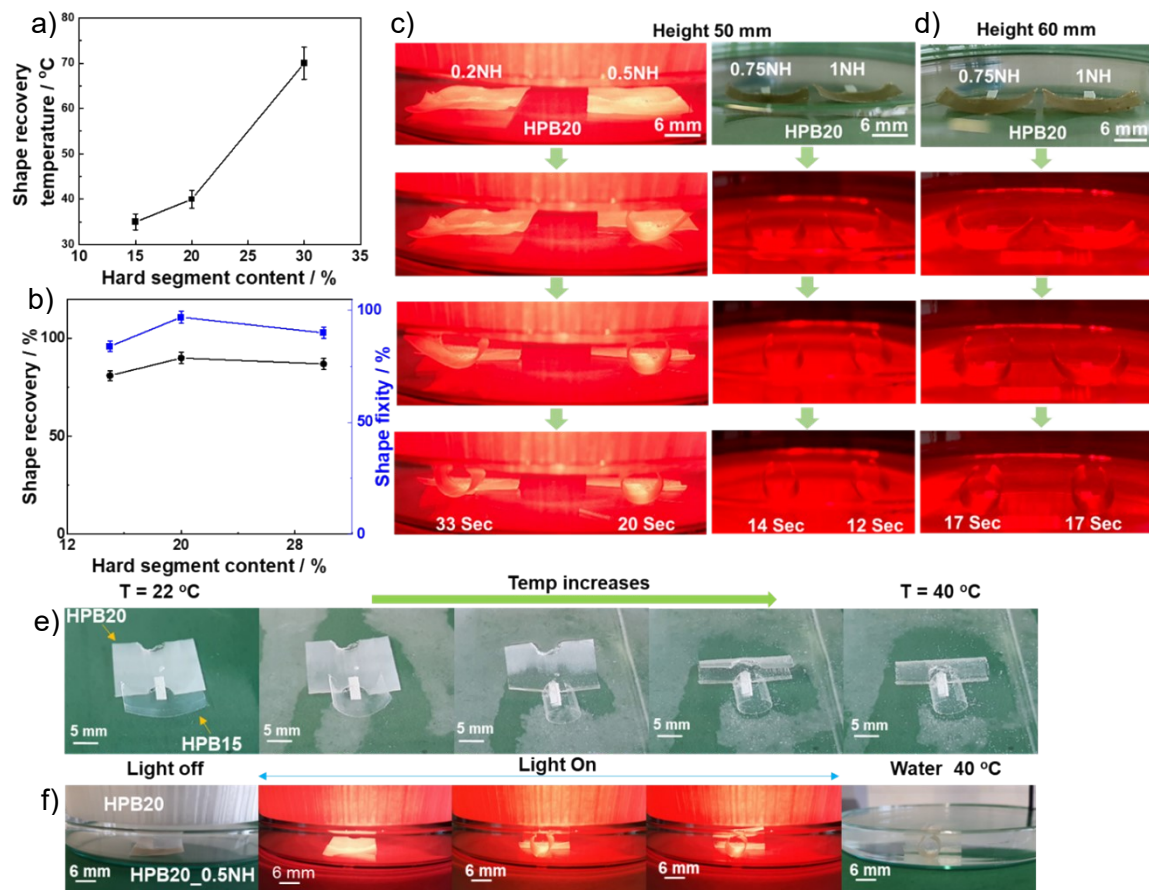


Figure S8: Demonstration of shape memory as well as folding behavior: a) Shape recovery behavior of different SMPUs has been investigated by exposing different programmed structures to heat. Shape recovery temperature increases with increasing the hard segment content (%); b) Shape recovery and fixity of different SMPUs increase with increasing HSC from 15 to 20 % and then decreases slightly for 30% HSC; c) The shape recovery profile with time of different nano hybrids has been investigated by exposing the programmed structures in near-infrared light. The recovery time decreases with increasing the concentration of the NPs in nano hybrids; d) While an increase in the distance between the light source and samples increases the recovery time; e) Demonstration of coordinated sequential folding of the programmed component 1 (made of HPB20) and component 2 (made of HPB15) with increasing temperature in order to achieve the

T-junction; f) Demonstration of coordinated sequential folding of the programmed component 1 (made of HPB20) and component 2 (made of HPB20_0.5NH) by exposing them first to near IR light and then temp to achieve the T-junction.

Video SV1: Demonstrating the 3D printing of the components of T-junction using a pneumatic pressure assisted melt extrusion-based 3D printer.

Video SV2: Demonstration of T-junction formation by heat-induced coordinated sequential folding of two components made of HPB20 (Component 1) and HPB15 (Component 2).

Video SV3: Demonstration of T-junction formation by near IR light triggered coordinated sequential folding of two components made of different nanohybrids (different shape recovery response).